https://doi.org/10.1016/j.apacoust.2017.09.026

Technical Note

Acoustic performance of different Helmholtz resonator array configurations

Chenzhi Cai and Cheuk Ming Mak *

Department of Building Services Engineering, The Hong Kong Polytechnic University, Hung Hom, Kowloon, Hong Kong, China

chenzhi.cai@connect.polyu.hk, cheuk-ming.mak@polyu.edu.hk

*Corresponding author.
E-mail Address: cheuk-ming.mak@polyu.edu.hk (C.M.Mak).
Telephone: +852 2766 5856
Fax: +852 2765 7198

Abstract

This paper presents a theoretical study of the acoustic performance of different Helmholtz resonator (HR) array configurations. A dual HR consisting of two HRs connected in series (neck-cavity-neck-cavity) could be considered as a serial HR array. Two HRs mounted on the same cross-section of the duct constitute a parallel HR array. A lined HR array is composed of two HRs installed on the longitudinal direction of the duct. Since HR is reactive silencer without energy consumption, the energy storage capacity (C_{TL}) of HR arrays could be defined as the area under transmission loss curve. The transfer matrix method is developed to conduct the investigation. The predicted theoretical results fit well with the Finite Element Method (FEM) simulation results. The results indicate that the installation methods have significant effects on transmission loss curves. However, the C_{TL} of the dual HR equals the C_{TL} of each single component HR mounted on the duct in despite of the dual HR having two HRs. The C_{TL} of the parallel HR array is equivalent to the C_{TL} of the lined HR array, which is twice the C_{TL} of the dual HR. The C_{TL} should therefore be considered as one of the main acoustic characteristics of a HR or an array and be taken into consideration in noise control optimization and HR design.

Keywords: Helmholtz resonator; transmission loss; energy storage capacity;

1. Introduction

An important application of a Helmholtz resonator (HR) that consists of a cavity communicating with an external duct through an orifice is the reduction of noise propagation in ducts. The resonance frequency of a HR is only determined by its geometries. It is therefore straightforward to design a HR with a desired resonance frequency. Owing to the characteristics of simplicity, adjustability and durability, the applications of the HR become an important area of study and have been utilized in numerous duct-structure systems, such as ventilation and air conditioning system in buildings, automotive duct systems and aero-engines, for the attenuation of noise produced by in-ducted elements [1-5].

Many researchers and engineers around the world have devoted their attention to the investigation of the HR. A lot of achievements have been made and are documented in numerous pieces of literature. Mainly through the labours of Helmholtz, Rayleight, Ingard, Sondhauss and Wertheim, the classical lumped approach for a HR is supposed to be analogous to the mechanical mass-spring system with end-correction factors for the sake of the accuracy [6]. Furthermore, a considerable number of researchers have developed the wave propagation in both the duct and the HR in theoretical analysis from an initial one-dimensional wave propagation approach to a multidimensional approach in order to account for nonplanar effects [7-9]. Since the HR is qualified as narrow band silencer and it is only effective at its resonance peak. Various modification forms of HRs have been studied in order to improve the acoustic performance of a HR. Chanaud [10] investigated the effects of different orifice shapes and cavity geometries on the resonance frequency of HR. Tang and Sirignano [7] showed that resonance frequency of a HR was reduced by

increasing the neck length. In order to lengthen the neck, an extended neck and a spiral neck were proposed by Selamet and Lee [11] and Shi and Mak [12] respectively. Cai et al. [13] compared the acoustic performance of HRs with these two types of necks. Tang [14] examined the HR with tapered necks of increasing cross-sectional area towards cavity both experimentally and theoretically. Griffin et al. [15] demonstrated the mechanically coupled HRs through a thin membrane to obtain three resonance frequencies instead of two. Xu et al. [16] derived expressions of two resonance frequencies and the transmission loss of a dual HR formed by a pair of neck and cavity connected in series.

However, there were no research literature regarding the HR's energy storage capacity until the recent work of Cai and Mak [17]. They proposed the concept of energy storage based on the transmission loss index. This paper focuses on evaluating the acoustic performance of different HR array configurations, especially the energy storage capacity of different HR arrays. Three different HR arrays are investigated here: 1) a dual HR consists of two HRs connected in series (neck-cavity-neck-cavity) could be considered as a serial HR array; 2) two HRs mounted on the same cross-section of the duct constitute a parallel HR array; 3) a lined HR array is composed of two HRs installed on the longitudinal direction of the duct. As low frequencies are the main concerns in this study, the frequency range considered here is well below the duct's cutoff frequency. Hence, only planar wave is assumed to propagate through the duct. The theoretical predictions are validated by Finite Element Method (FEM) simulation. It is hoped that the analysis of energy storage capacity could contribute to the noise control optimization and the HR design.

2. Theoretical analysis of different Helmholtz resonator arrays

The sound fields inside a HR are clearly multidimensional because of sudden discontinuities area [8]. However, on the basis of low frequency range of interest in this paper, the dimensions of HRs considered here are significant small compared to the wavelengths. It is therefore that the evanescent high-order modes can be considered by introducing an end correction factor to improve the accuracy of the classical lumped approach. The effect of viscous dissipation through the necks will be ignored for simplicity.

2.1 A single Helmholtz resonator

Although a multidimensional approach provides a more accurate measure of the acoustics impedance of a HR, the main purpose here is to reveal the energy storage capacity of a HR. For this reason, the classical lumped approach is adopted here and the evanescent high-order modes are considered by introducing an end correction factor to improve the accuracy. It is therefore that the acoustic impedance of a HR is given as:

$$Z_r = j\frac{\rho_0 l_n'}{S_n \omega}(\omega^2 - \omega_0^2) \tag{1}$$

where ρ_0 is air density, l_n' and S_n are the neck's effective length and area respectively, $\omega_0 = c_0\sqrt{S_n / l_n' V_c}$ (V_c is the cavity volume and c_0 is the speed of sound in the air) and ω are the resonant circular frequency and circular frequency respectively.

Once the acoustic impedance is obtained, the transmission loss of a side-branch HR mounted on a duct with cross-sectional area S_d could be expressed as:

$$TL = 20\log_{10}\left(\frac{1}{2}\left|2 + \frac{\rho_0 c_0}{S_d}\frac{1}{Z_r}\right|\right) \tag{2}$$

2.2 A dual Helmholtz resonator

A dual HR formed by two HRs connected in series (neck-cavity-neck-cavity), which could be considered as a serial HR array, leads to two resonance frequencies. A dual HR could be analogous to a two degrees of freedom mechanical system, as illustrated in Fig. 2. According to Hooke's law, it should be noted that the first string has different stiffness (K_{11} and K_{12}) to the front and rear masses connected on it. By applying the Newton's second law of motion to the first mass M_1 and the second M_2 respectively yield:

$$M_1 \frac{d^2 x_1}{dt^2} + R_1 \frac{dx_1}{dt} + K_{11} x_1 = S_1 p_0 e^{j\omega t}, \; M_2 \frac{d^2 x_2}{dt^2} + R_2 \frac{dx_2}{dt} + K_{22} x_2 = K_{12} x_2 \tag{3}$$

where $M_1 = \rho_0 S_1 l_{n1}'$ and $M_2 = \rho_0 S_2 l_{n2}'$ are the corresponding mass of air in the necks including the end-correction factor, R_1 and R_2 are damping coefficients of necks, K_{11} and K_{12} represent the stiffness of the first spring to the first mass and second mass respectively, $K_{22} = \rho_0 c_0^2 {S_2}^2 / V_2$ is the stiffness of the second spring, $e^{j\omega t}$ is the time-harmonic disturbance. Appling the Hooke's law to the mechanical analogy of a dual HR, the stiffness K_{11} and K_{12} could be obtained as:

$$K_{11} = \frac{\rho_0 c_0^2 S_1}{V_1 x_1}(S_1 x_1 - S_2 x_2), \qquad K_{12} = \frac{\rho_0 c_0^2 S_2}{V_1 x_2}(S_1 x_1 - S_2 x_2) \tag{4}$$

With the introduction of Eq. (4), Eq. (3) could be rewritten as:

$$\begin{cases} M_1 \dfrac{d^2 x_1}{dt^2} + R_1 \dfrac{dx_1}{dt} + \dfrac{\rho_0 c_0^2 S_1}{V_1}(S_1 x_1 - S_2 x_2) = S_1 p_0 e^{j\omega t} \\ M_2 \dfrac{d^2 x_2}{dt^2} + R_2 \dfrac{dx_2}{dt} + \dfrac{\rho_0 c_0^2 S_2^2}{V_1} x_2 - \dfrac{\rho_0 c_0^2 S_2}{V_1}(S_1 x_1 - S_2 x_2) = 0 \end{cases} \tag{5}$$

Substituting $x_1 = X_1 e^{j\omega t}$ and $x_2 = X_2 e^{j\omega t}$ into Eq. (5) and rearranging in the matrix form as:

$$\begin{bmatrix} -\omega^2 M_1 + j\omega R_1 + \dfrac{\rho_0 c_0^2 S_1^2}{V_1} & -\dfrac{\rho_0 c_0^2 S_1 S_2}{V_1} \\ -\dfrac{\rho_0 c_0^2 S_1 S_2}{V_1} & -\omega^2 M_2 + j\omega R_2 + \rho_0 c_0^2 S_2^2 \dfrac{(V_1+V_2)}{V_1 V_2} \end{bmatrix} \begin{Bmatrix} X_1 e^{j\omega t} \\ X_2 e^{j\omega t} \end{Bmatrix} = \begin{Bmatrix} S_1 p_0 e^{j\omega t} \\ 0 \end{Bmatrix} \quad (6)$$

where X_1 and X_2 are the magnitude of the first and the second neck's displacement respectively. Eq. (6) could be simplified as:

$$\begin{bmatrix} a_{11} & a_{12} \\ a_{21} & a_{22} \end{bmatrix} \begin{Bmatrix} X_1 \\ X_2 \end{Bmatrix} = \begin{Bmatrix} p_0 S_1 \\ 0 \end{Bmatrix} \quad (7)$$

where $\begin{bmatrix} -\omega^2 M_1 + j\omega R_1 + \dfrac{\rho_0 c_0^2 S_1^2}{V_1} & -\dfrac{\rho_0 c_0^2 S_1 S_2}{V_1} \\ -\dfrac{\rho_0 c_0^2 S_1 S_2}{V_1} & -\omega^2 M_2 + j\omega R_2 + \rho_0 c_0^2 S_2^2 \dfrac{(V_1+V_2)}{V_1 V_2} \end{bmatrix} = \begin{bmatrix} a_{11} & a_{12} \\ a_{21} & a_{22} \end{bmatrix}$.

According to Eq. (7), the relation of X_1 and $p_0 S_1$ could be described as $X_1 = p_0 S_1 a_{22} / (a_{11} a_{22} - a_{12} a_{21})$. It is therefore that the acoustic impedance of the dual HR could be obtained as:

$$Z_r = \frac{p_0}{j\omega X_1 S_1} = \frac{1}{j\omega S_1^{\,2}} \frac{a_{11} a_{22} - a_{12} a_{21}}{a_{22}} \quad (8)$$

By ignored the effect of viscous dissipation through the necks for simplicity ($R_1 = R_2 = 0$), Eq.(8) could be rewritten as:

$$Z_r = \frac{1}{j\omega S_1^{\,2}} \frac{M_1 M_2 \omega^4 - \rho_0 c_0^2 [M_1 S_2^2 (\frac{1}{V_1} + \frac{1}{V_2}) + M_2 S_1^2 \frac{1}{V_1}] \omega^2 + \dfrac{\rho_0^{\,2} c_0^4 S_1^{\,2} S_2^{\,2}}{V_1 V_2}}{\rho_0 c_0^2 S_2^2 (\frac{1}{V_1} + \frac{1}{V_2}) - M_2 \omega^2} \quad (9)$$

It is therefore that the transmission loss of the dual HR could be obtained through Eq. (2).

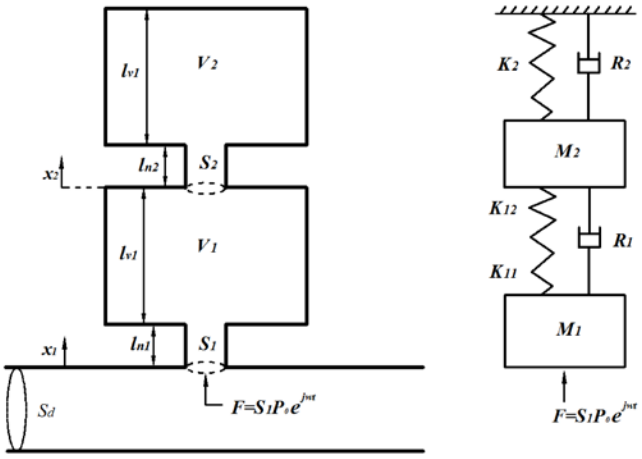

Fig. 1 Mechanical analogy of a dual Helmholtz resonator

2.3 A parallel Helmholtz resonator array

Two Helmholtz resonators mounted on the same cross-section of the duct is illustrated in Fig. 2. The acoustic impedance of these two HRs can be calculated by Eq. (1), expressed as Z_{r1} and Z_{r2} respectively. The continuity conditions of sound pressure and volume velocity at the duct-neck interface give:

$$p_1 = p_2 = p_{f1} = p_{f2},\ S_d u_1 = S_d u_2 + \frac{p_{f1}}{Z_{r1}} + \frac{p_{f2}}{Z_{r2}} \tag{10}$$

where p with subscript represents sound pressure, u_1 and u_2 are the particle velocity at point 1 and point 2 respectively.

The relation between point 1 and to point 2 could be obtained by combining the continuity conditions as:

$$\begin{bmatrix} p_1 \\ \rho_0 c_0 u_1 \end{bmatrix} = \begin{pmatrix} 1 & 0 \\ \dfrac{\rho_0 c_0}{S_d}\dfrac{Z_{r1}+Z_{r2}}{Z_{r1}Z_{r2}} & 1 \end{pmatrix} \begin{bmatrix} p_2 \\ \rho_0 c_0 u_2 \end{bmatrix} \tag{11}$$

Then the transmission loss of the parallel HR array can be determined by the four-pole parameters method as [18]:

$$TL = 20\log_{10}\left(\frac{1}{2}\left|2+\frac{\rho_0 c_0}{S_d}\frac{Z_{r1}+Z_{r2}}{Z_{r1}Z_{r2}}\right|\right) \tag{12}$$

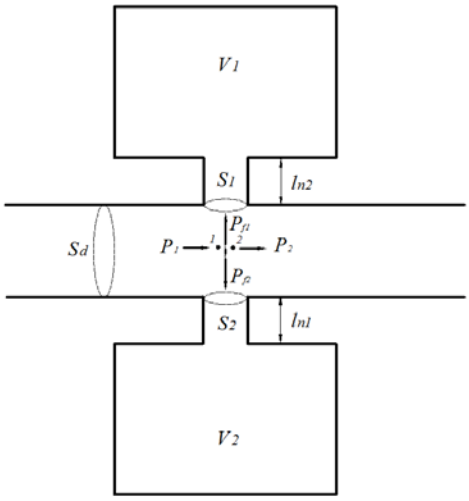

Fig. 2 A parallel Helmholtz resonator array

2.4 A lined Helmholtz resonator array

A single HR has a high transmission loss peak with narrow band at its resonance frequency. Combining several HRs in line is a possible way to obtain a broader noise attenuation band. Fig. 3 demonstrates an array of two lined HRs mounted on the duct. Similar to Eq. (11), by combining the continuity conditions of the sound pressure and volume velocity at neck-neck interfaces, the relation between point 1 and point 2 and that between point 3 to point 4 could be obtained respectively as:

$$\begin{bmatrix} p_1 \\ \rho_0 c_0 u_1 \end{bmatrix} = \begin{pmatrix} 1 & 0 \\ \frac{\rho_0 c_0}{S_d}\frac{1}{Z_{r1}} & 1 \end{pmatrix} \begin{bmatrix} p_2 \\ \rho_0 c_0 u_2 \end{bmatrix} = \mathbf{T}_{r1} \begin{bmatrix} p_2 \\ \rho_0 c_0 u_2 \end{bmatrix} \tag{13}$$

$$\begin{bmatrix} p_3 \\ \rho_0 c_0 u_3 \end{bmatrix} = \begin{pmatrix} 1 & 0 \\ \frac{\rho_0 c_0}{S_d}\frac{1}{Z_{r2}} & 1 \end{pmatrix} \begin{bmatrix} p_4 \\ \rho_0 c_0 u_4 \end{bmatrix} = \mathbf{T}_{r2} \begin{bmatrix} p_4 \\ \rho_0 c_0 u_4 \end{bmatrix} \tag{14}$$

Only the planar wave is assumed to propagate through the duct due to the interest of low-frequency range here. It means that there is only a phase delay of the wave propagation in the straight duct from point 2 to point 3. Thus, the relation of point 2 and point 3 could be described as:

$$\begin{bmatrix} p_2 \\ \rho_0 c_0 u_2 \end{bmatrix} = \begin{pmatrix} \cos(kL) & j\sin(kL) \\ j\sin(kL) & \cos(kL) \end{pmatrix} \begin{bmatrix} p_3 \\ \rho_0 c_0 u_3 \end{bmatrix} = \mathbf{T}_{duct} \begin{bmatrix} p_3 \\ \rho_0 c_0 u_3 \end{bmatrix} \tag{15}$$

where L represents the distance between two HRs, $\mathbf{T}_{duct}$ is the transfer matrix of the straight duct, k is the number of wave. Then, the relation of point 1 and point 4 could be described in the matrix form as:

$$\begin{bmatrix} p_1 \\ \rho_0 c_0 u_1 \end{bmatrix} = \mathbf{T}_{r1}\mathbf{T}_{dcut}\mathbf{T}_{r2} \begin{bmatrix} p_4 \\ \rho_0 c_0 u_4 \end{bmatrix} = \begin{bmatrix} t_{11} & t_{12} \\ t_{21} & t_{22} \end{bmatrix} \begin{bmatrix} p_4 \\ \rho_0 c_0 u_4 \end{bmatrix} \tag{16}$$

Once the transfer matrix $\mathbf{T}_{r1}\mathbf{T}_{dcut}\mathbf{T}_{r2}$ has been obtained, the transmission loss of the lined HR array can be calculated from the expression as:

$$TL = 20\log_{10}\left(\frac{1}{2}\left|t_{11} + t_{12} + t_{21} + t_{22}\right|\right) \tag{17}$$

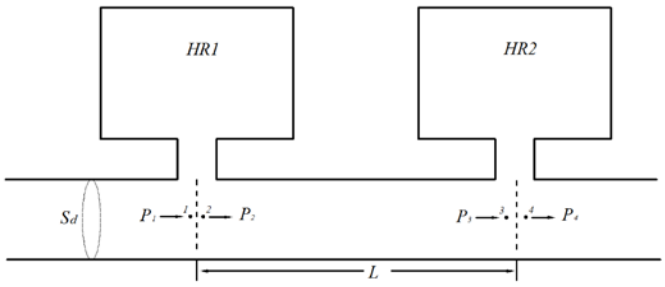

Fig. 3 Schematic diagram of a lined Helmholtz resonator array

2.5 Energy storage capacity

The transmission loss index is used to evaluate acoustic transmission performance in the frequency domain. However, it cannot be used to analyze the attenuation characteristics

quantitatively. The concept of energy storage capacity, which is based on the transmission loss index, could give us a distinct parameter to evaluate the noise attenuation performance and ability of a single HR or an array. Since HRs are reactive silencers without energy consumption, the energy storage capacity C_{TL} of a HR array is defined as the integration of transmission loss TL and is expressed as:

$$C_{TL} = \int TL df = \sum_{i=0}^{f} TL_i (f_{i+1} - f_i) \tag{18}$$

The energy storage capacity could be considered as one of the main acoustic characteristics of a single HR or a HR array. Moreover, the quantitative parameter C_{TL} could be adopted in the noise control optimization and HR design to evaluate the acoustic performance.

3. Results and discussion

3.1 Validation of the predicted transmission loss of the dual Helmholtz resonator

The dual HR could be considered as two HRs connected in series (neck-cavity-neck-cavity), as illustrated in Fig. 1. There are two kinds of HRs with same neck dimensions and different cavity volumes are adopted here, annotated as HR1 and HR2 respectively. The geometries of HRs used in this paper are: same neck area $S_n = 2.25\pi cm^2$ and neck length $l_n = 2.5cm$, cavity volume $V_{R1} = 653.4\pi cm^3$ and $V_{R2} = 261.36\pi cm^3$ corresponding to HR1 and HR2 respectively. The cross-sectional area of the main duct is $S_d = 25cm^2$ .The resonance frequency of a HR is only determined by its geometries. It is therefore that the resonance frequencies of HR1 and HR2 are 152 Hz and 244 Hz respectively. Fig. 4 illustrates the configuration of two dual HR cases: HR1-HR2 model and HR2-HR1 model respectively.

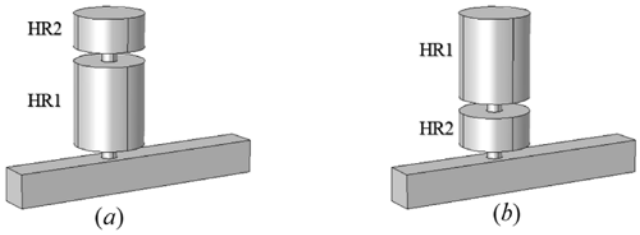

Fig. 4 Configuration of two dual HR cases: (a) HR1-HR2 model, (b) HR2-HR1 model

The predicted transmission loss of these two cases are compared with two individual HRs, as shown in Fig. 5. It can be observed that the dual HR cases have two resonance frequencies. The first resonance frequency of HR1-HR2 model and HR2-HR1 model are 121 Hz and 103 Hz respectively, which are both lower than 152 Hz (HR1's resonance frequency). The second resonance frequency of HR1-HR2 model and HR2-HR1 model are 301 Hz and 361 Hz, which are both higher than 244 Hz (HR2's resonance frequency). The HR2-HR1 model could provide a lower first resonance frequency than the HR1-HR2 model, however, the decreased first resonance frequency compromises an increasing second resonance frequency. The comparison of the analytical predicted results and the FEM simulation results are illustrated in Fig. 6, and the prediction results are in good agreement with the FEM simulation results.

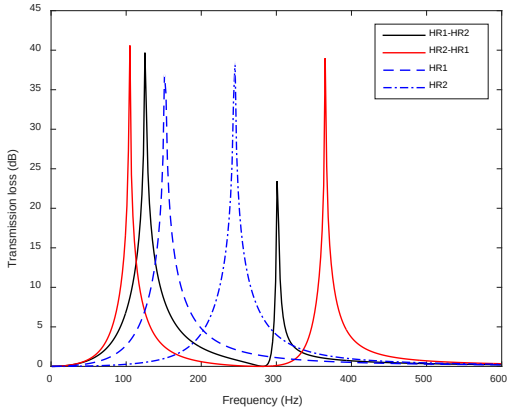

Fig. 5 Transmission loss of dual HR cases and individual HRs

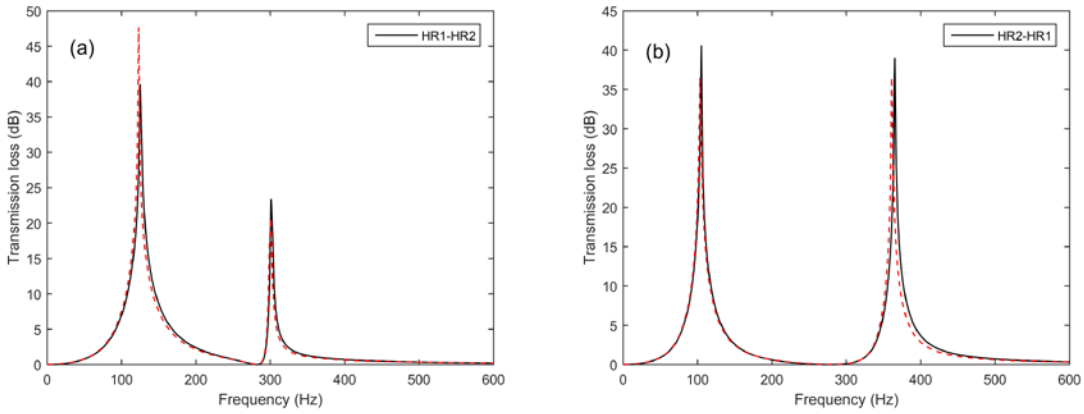

Fig. 6 Comparison of the analytical predictions and the FEM simulation in respect of different dual HR models (solid lines represent the theoretical predictions, and dashed lines represent the FEM simulation results)

3.2 Validation of the predicted transmission loss of parallel Helmholtz resonator array

The parallel HR array consisting of two HRs mounted on the same cross-section of the duct is shown in Fig. 2. The two kinds of HRs used here are the same as HR1 and HR2 above, as is as the cross-section area of main duct. On the basis of low-frequency range considered in this paper, only planar wave is assumed to propagate in the duct. It is therefore that these two HRs can be mounted on arbitrary side of the cross-section of the duct [19]. Fig. 7 compares the transmission loss between the parallel HR array and each HR. The parallel HR array has two resonance frequencies with nearly the same peak amplitudes corresponding to each HR's resonance frequency and peak amplitude. There is also a frequency at the intersection of two individual HRs' *TL* curve, suggesting as an anti-resonance behavior. A good agreement between the theoretical predicted *TL* results and the FEM simulation results can also be seen in Fig. 8. The parallel HR array could be approximated as the superposition of two individual HRs' *TL* curve.

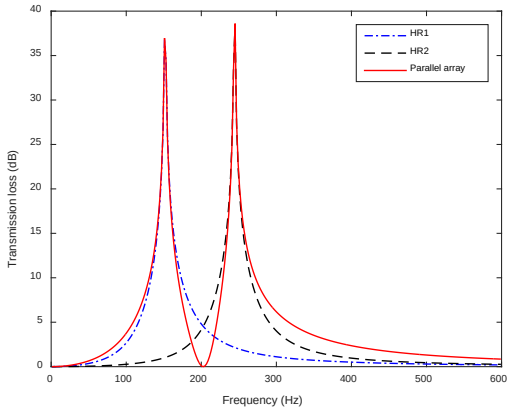

Fig. 7 Transmission loss of the parallel HR array and individual HRs

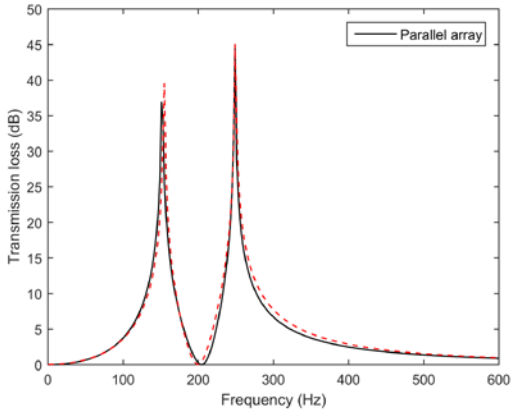

Fig. 8 Comparison of the analytical predictions and the FEM simulation in respect of the parallel HR array (solid line represents the theoretical predictions, and dashed line represents the FEM simulation results)

3.3 Validation of the predicted transmission loss of the lined Helmholtz resonator array

The schematic diagram of a lined Helmholtz resonator array, which is composed of two HRs, is exhibited in Fig. 3. The used HRs (HR1 and HR2) and the main duct are the same as mentioned above. The optimal distance is corresponding to the quarter-wavelength of HRs' mean frequency defined as $f_m=2f_{HR1}* f_{HR2}/(f_{HR1}+ f_{HR2})$ [20]. As a consequence, the distance L between two HRs used in this paper is $L = 0.46m$. The comparison of theoretical predicted transmission loss between the lined HR array and each HR is shown in Fig. 9.

Two peak amplitudes corresponding to each HR's resonance frequency could be observed from the lined HR array. Moreover, the lined HR array provides a much broader noise attenuation band between the resonance frequencies of these two HRs. Fig. 10 shows that the theoretical predicted results fit well with the FEM simulation results.

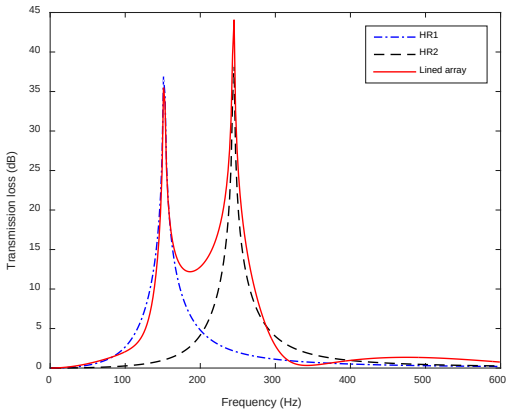

Fig. 9 Transmission loss of the lined HR array and individual HRs

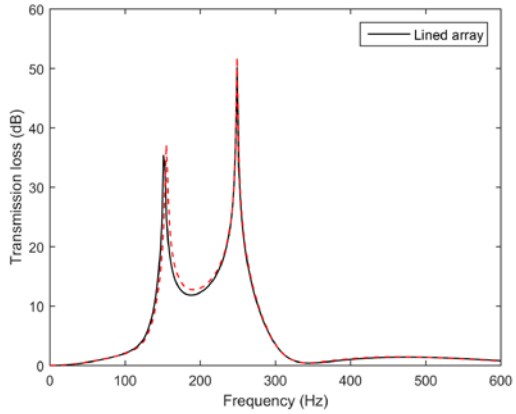

Fig. 10 Comparison of the analytical predictions and the FEM simulation in respect of the lined HR array (solid line represents the theoretical predictions, and dashed line represents the FEM simulation results)

3.4 Comparison of noise attenuation capacity

The energy storage capacity C_{TL} of those cases as described above is exhibited in Table 1. The maximum relative errors of C_{TL} between the theoretical analysis and FEM simulation are less than 5% in frequency range of 0~600 Hz (parallel case) and less than 1% in frequency range of 0~1000 Hz respectively. It should be noted that the C_{TL} of HR1 equals to the C_{TL} of HR2. It means that the change of the cavity volume has no effect on the C_{TL}. It only alters the resonance frequency. It should be noted that although the dual HR contains two HRs, the C_{TL} of the dual HR equals to the C_{TL} of each single component HR mounted on the ducted. The added HR in series leads to two resonance frequencies, however, these two noise attenuation bands compromises with a narrower noise attenuation band. Besides, being bulky is another disadvantage for a dual HR when compared with its component HRs.

Although the transmission loss performance of the lined HR array is different from the parallel array, as depicted in Fig. 11. The parallel array could be approximated as the combination of the transmission loss performance of HR1 and HR2, as illustrated as Fig. 7. The lined HR array could provide a much broader noise attenuation band between two resonance frequencies. However, the C_{TL} of the parallel HR array equals to the C_{TL} of the lined HR array, which is twice the C_{TL} of the dual HR cases. The lined HR array and the parallel HR array demand the same space as the dual HR, but in different ways.

Table 1. C_{TL} with different frequency range

	C_{TL} with different frequency range			
	0~600 Hz		0~1000 Hz	
Cases	Theory	FEM	Theory	FEM
HR1	1.622×10^3	1.625×10^3	1.647×10^3	1.644×10^3
HR2	1.627×10^3	1.633×10^3	1.659×10^3	1.66×10^3
HR1-HR2	1.631×10^3	1.626×10^3	1.669×10^3	1.671×10^3

HR2-HR1	1.641×10^3	1.644×10^3	1.664×10^3	1.674×10^3
Parallel array	3.012×10^3	3.129×10^3	3.216×10^3	3.286×10^3
Lined array	3.164×10^3	3.239×10^3	3.249×10^3	3.279×10^3

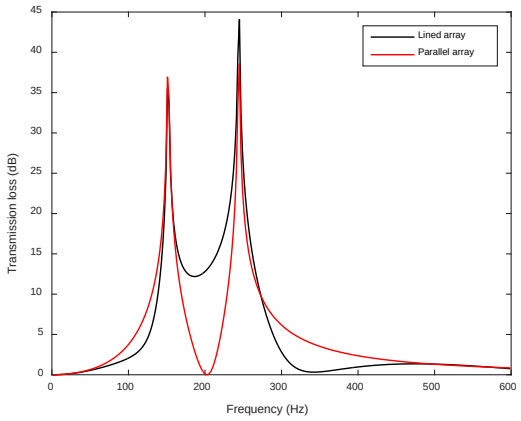

Fig. 11 Transmission loss of the lined HR array and the parallel HR array

4. Conclusion

The acoustic performance of three kinds of HR arrays are investigated theoretically and numerically. The dual HR consist of two HRs connected in series is considered as a serial HR array. Two HRs mounted on the same cross-section of the duct constitute a parallel HR array. The lined HR array is composed of two HRs installed on the longitudinal direction of the duct. Different installation methods have significant effects on *TL* performance. The dual HR could provide two resonance frequencies, which the first and second resonance frequency are lower and higher than the resonance frequency of any component HRs respectively. By altering the connected sequence of two HRs in the dual HR, the reduced first resonance frequency compromises an increasing second resonance frequency could be observed. The parallel HR array has two resonance frequencies with nearly the same peak amplitudes corresponding to each HR's resonance frequency and peak amplitude. It could be approximated as the superposition of two individual HRs' *TL* curve. The lined

HR array provides a much broader noise attenuation band between the resonance frequencies of these two HRs. The two resonance frequencies corresponding to each HR's resonance frequency could also be observed. In consideration of energy storage capacity, it should be noted the C_{TL} of the dual HR equals to the C_{TL} of each single component HR mounted on the ducted. The C_{TL} of the parallel HR array equals the C_{TL} of the lined HR array, which is twice the C_{TL} of the dual HR or each component HR. In addition, a dual HR is bulky when compared with its component HRs. The lined HR array and the parallel HR array demand the same space as the dual HR, but in different ways. It is therefore the C_{TL} should be considered as one of the main acoustic characteristics to evaluate the attenuation efficiency of HR arrays. The quantitative parameter C_{TL} has potential applications to be used in the noise control optimization and HR design to evaluate the acoustic performance.

Acknowledgements

The work described in this paper was fully supported by a grant from the Research Grants Council of the Hong Kong Special Administrative Region, China (Project No. PolyU 152116/14E).

References

[1]Müller Gehard, Möser Michaël. Handbook of Engineering Acoustics. Spiniger: Verlag; 2013.

[2] Munjal ML. Acoustics of Ducts and Muffers. New York: Wiley, 1987.

[3] Mak CM, Wang Z. Recent advances in building acosutics: An overviwe of prediction methods and their applications. Build Environ 2015;91:118-126.

[4] Mak CM, Yang J. A prediction method for aerodynamic sound produced by closely space element in air ducts. J Sound Vib 2000;229(3):743-753.

[5] Mak CM. Development of a prediction method for flow-generated noise produced by duct elements in ventilation systems. Appl Acoust 2002;63(1):81-93.

[6] Beyer RT. Sounds of Our Times: Two Hundred Years of Acoustics. Spiniger: Verlag; 1999.

[7] Tang PK, Sirignano WA. Theory of a generlized Helmholtz resoator. J Acoust Soc Am 1973;26(2):247-262.

[8] Sahasrabudhe AD, Munjal ML and Anantha Ramu S. Anlysis of interance due to the higher order mode effecs in a sudden area discontinuity. J Sound Vib 1995;185(3):515-529.

[9] Selamet A, Ji ZL. Circular asymmetric Helmholtz resonators. J Acoust Soc Am 2000;107(5):2360-2369.

[10] Chanaud RC. Effects of geometry on the resonance frequrncy of Helmholtz resonator. J Sound Vib 1994;178(3):337-348.

[11] Selamet A, Lee IJ. Helmholtz resonator with extended neck. J Acoust Soc Am 2003;113(4):1975-1985.

[12] Shi XF, Mak CM. Helmholtz resonator with a spiral neck. Appl Acoust 2015;99:68-71.

[13] Cai C, Mak CM, Shi X. An extended neck versus a spiral neck of the Helmholz resonator. Appl Acoust 2017;115:74-80.

[14] Tang SK. On Helmholtz resonators with tapered necks. J Sound Vib 2005;279(3-5):1085-1096.

[15] Griffin S, Lane SA, Huybrechts S. Coupled Helmholtz resonators for acosutic attenatuion. J Vib Acoust 2001;123:11-17.

[16] Xu MB, Selamet A, Kim H. Dual Helmholtz resonator. Appl Acoust 2010;71:822-829.

[17] Cai C, Mak CM. Noise control zone for a periodic ducted Helmholtz resonator system. J Acoust Soc Am 2016;140(6):EL471-EL477.

[18] ZL Ji, JZ Sha. Four-pole parameters of a duct with Low Mach number flow. J Acoust Soc Am 1995;98(5):2848-2850.

[19] Cai C, Mak CM, Wang X. Noise attenaution perforamnce improvement by adding Helmholtz resonators on the periodic ducted Helmholtz resonator systems. Appl Acoust 2017;122:8-15.

[20] Seo SH, Kim YH. Silencer design by using array resonators for low-freqeuncy band noise reduction. J Acoust Soc Am 2005;118(4):2332-2338.

Figure captions

Fig. 1 Mechanical analogy of a dual Helmholtz resonator

Fig. 2 A parallel Helmholtz resonator array

Fig. 3 Schematic diagram of a lined Helmholtz resonator array

Fig. 4 Configuration of two dual HR cases: (a) HR1-HR2 model, (b) HR2-HR1 model

Fig. 5 Transmission loss of dual HR cases and individual HRs